Turkish Journal of Electrical Engineering & Computer Sciences

http://journals.tubitak.gov.tr/elektrik/

Research Article

Turk J Elec Eng & Comp Sci
(2018) 26: 1871 – 1880
© TÜBİTAK
doi:10.3906/elk-1708-48

Novel low-loss microstrip triplexer using coupled lines and step impedance cells for 4G and WiMAX applications

Abbas REZAEI[1], **Leila NOORI**[2,*]
[1]Department of Electrical Engineering, Kermanshah University of Technology, Kermanshah, Iran
[2]Young Researchers and Elite Club, Kermanshah Branch, Islamic Azad University, Kermanshah, Iran

Received: 04.08.2017 • **Accepted/Published Online:** 03.04.2018 • **Final Version:** 27.07.2018

Abstract: In this paper, a new microstrip triplexer with flexible resonance frequencies is designed based on the properties of coupled lines, steps, and spiral cells. It operates at 2.67 GHz for 4G LTE and at 3.1 GHz and 3.43 GHz for IEEE 802.16 WiMAX. The close resonance frequencies make it suitable for frequency division duplex applications. In order to improve insertion loss, the LC equivalent circuit of the proposed resonator is analyzed. Moreover, careful alignment of the coupled lines and step impedance structures is performed to improve the insertion and return losses so that they are 0.72/0.63/0.81 dB and 24.5/24/24.7 dB, respectively. The frequency response shows good selectivity for each channel. Meanwhile, there are several transmission zeros above the first channel and below the last one that improve the stopband properties. The proposed triplexer is fabricated and measured. The simulation and measurement results are in good agreement, which validates the introduced methodology.

Key words: Microstrip, triplexer, WiMAX, return loss, insertion loss

1. Introduction

Planar microstrip diplexers and multiplexers are widely used in modern mobile communication and wireless systems [1,2]. They can separate signals that are close together and they can select the desired frequency ranges in crowded frequency bands. Strong demands for compact planar multiplexers with high performance encourage designers to provide various structures for communication services, where many users utilize close frequency bands. A triplexer is a multiplexer with three channels to select the frequencies of interest. In [3], a microstrip triplexer composed of matching cells, a stepped-impedance structure, parallel-coupled lines, and hairpin and open-loop resonators was presented. Despite its large return loss and weak frequency selectivity, a significant reduction in the insertion losses could be seen. Although the low insertion loss at resonance frequency is an important issue, most of the reported triplexers could not reduce it [4–18]. These triplexers have been designed using various microstrip structures. Coupled open-loop resonators and coupled lines were used to obtain high isolation in [4]. In [5], hairpin structures were employed to achieve three controllable resonance frequencies. However, the return losses at all passbands were not good enough. Despite the fact that compact structures are a requirement of modern wireless systems, some previous works did not have practical solutions to reduce the size [6–9]. In [6], the step impedance units as matching networks were utilized for integrating main resonators so that a high selectivity frequency response could be obtained. The microstrip triplexer reported in [7] was designed using open-loop resonators. It resonates at 1.8 GHz for digital communication systems, 3.2 GHz for

*Correspondence: leila_noori62@yahoo.com

WiMAX, and 4.4 GHz for C-band applications. In [8], third-order parallel-coupled bandpass resonators were integrated to design a wide stopband triplexer. In [9], a star junction cell was connected to microstrip hairpin cells to realize wide fractional bandwidths. Another common disadvantage of the previous triplexers is their high return losses [8–16]. In [10], a compact microstrip triplexer with three channels (2.15/2.95/3.80 GHz) was introduced based on mixed couplings of asymmetric split-ring resonators. In [11], high isolation was obtained by parallel-coupled lines and U-shape structures. In [12], one lowpass and two bandpass channels were created by T-shape, U-shape, and hairpin cells. In [13], compact coupled lines and radial structures were employed to achieve three channels at 1.2, 1.8, and 2.4 GHz. The microstrip triplexers designed in [14] and [15] improved the insertion losses partially. Having close resonance frequencies is an advantage of a well-designed triplexer. However, most of the reported triplexers do not have channels that are close enough to each other [3,5–10,12–15]. In [16], a fully integrated triplexer with close channels and large implementation area was proposed for multiband ultrawideband radio applications. Using meandered loop resonators, a microstrip triplexer was designed in [17]. Similar to the introduced triplexers in [4] and [7], it has one transmission pole in each channel with large insertion and return losses at all channels. Three bandpass filters were integrated by a circular junction to obtain a microstrip triplexer in [18]. In this structure, the middle band is undesired while it has large losses at all channels. Moreover, it occupies a large area and the selectivity of the first channel is low. The proposed triplexer in [19] has a transmission pole in each channel but it has large losses, large size, and poor isolation between ports 2 and 4. Another weakness of the designed triplexer in [19] is having undesired S_{21} at the last passband so that the harmonics of the first channel are not well attenuated in the third passband.

In this paper, a planar microstrip triplexer is designed using coupled lines and step impedance cells. It operates at close resonance frequencies of 2.67 GHz for 4G and 3.1 GHz and 3.43 GHz for IEEE 802.16 WiMAX, covering a frequency band of 3.17 GHz to 4.2 GHz. The main purpose is to decrease the losses while the channels are quite close together. Hence, we select a single mode resonator and then the conditions to obtain low loss are calculated mathematically. This is an important achievement because improving the losses when channels are close together is difficult. The designing method is organized as follows: first, a resonator is proposed and its LC equivalent circuit is obtained. Then a theoretical method is introduced based on the LC model to minimize the insertion loss at a desired resonance frequency. Next, the proposed resonators are integrated to complete the triplexer design. Finally, the obtained triplexer is optimized to reduce the size, return loss, and insertion loss simultaneously.

2. Triplexer design

As shown in Figure 1a, coupled lines loaded by step impedance structures are utilized to create a resonator. This basic structure can be used to design a triplexer. The input impedances of steps are depicted by Z_1 and Z_2 and the input impedances of stubs connected to port 1 and port 2 are shown by Z_3 and Z_4, respectively. Figure 1b shows an equivalent LC circuit of the coupled lines. To characterize the LC circuit of the coupled lines we divide it into four parts [20], which are presented in Figures 1a and 1b with the numbers 1, 2, 3, and 4. In the LC model, L_C demonstrates the coupling between lines. Furthermore, the equivalent circuit of each part of the coupled lines includes L_e and C_e. Figure 1c indicates a perfect equivalent LC circuit of the proposed resonator, where the equivalent LC model of steps and microstrip lines is also replaced. Since the effect of bends and steps is significant at frequencies higher than 10 GHz, their effects are not important. Therefore, the steps with characteristic impedances Z_1 and Z_2 are replaced by inductor L_1 and capacitor C_1 for Z_1 and inductor L_2 and capacitor C_2 for Z_2. As shown in Figure 1c, impedances of the stubs attached to port 1 and port 2

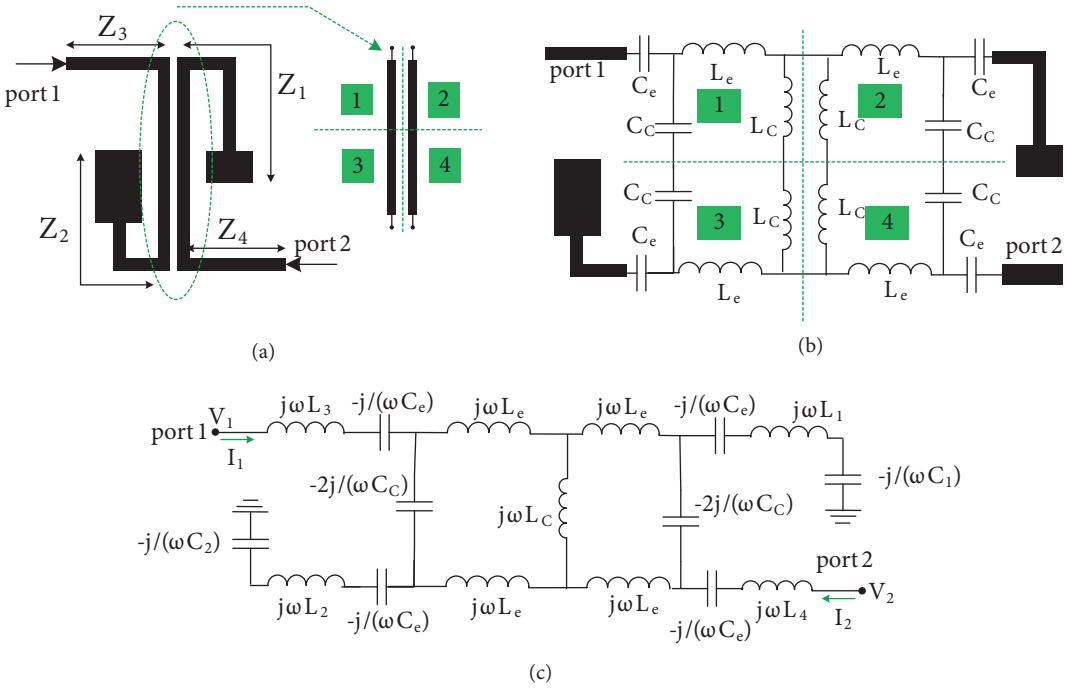

Figure 1. (a) Proposed resonator; (b) replacing the LC model of coupled lines; (c) perfect LC model of the proposed resonator.

are $j\omega L_3$ and $j\omega L_4$, respectively, where $\omega = 2\pi f_r$ and f_r is a resonance frequency. Since the insertion loss is calculated by $IL = -20\log(S_{21})$ or $IL = -20\log(S_{12})$, to minimize it S_{21} and S_{12} should be near 1. On the other hand, Z_{21} can be written as a function of S-parameters as follows [21]:

$$Z_{21} = \frac{2S_{21}Z_0}{(1-S_{11})(1-S_{22}) - S_{21}S_{21}} \tag{1}$$

Here, Z_o is the terminal impedance. It can be recognized that for obtaining the minimum value of insertion loss we must set $S_{21} = S_{12} = 1$. Accordingly, Eq. (1) can be summarized as follows.

$$Z_{21} = \frac{2Z_0}{(1-S_{11})(1-S_{22}) - 1} \tag{2}$$

Moreover, Z_{21} can be calculated from the LC equivalent circuit of the proposed resonator as follows.

$$Z_{21} = \frac{V_2}{I_1}|I_2 = \frac{Z_a Z_b Zc}{Z_R + 2Z_a + 2Z_b + Z_c} + \frac{Z_a Z_b}{Z_R + Z_a} + Z_d$$

where:

$$Z_a = \frac{-2j}{\omega C_C}$$

$$Z_b = j\omega L_e \tag{3}$$

$$Z_c = j\omega\, L_c$$

$$Z_d = j(\omega\, L_2 - \tfrac{1}{\omega\, C_2} - \tfrac{2}{\omega\, C_C})$$

$$\omega = 2\pi f_r$$

$$Z_R = \tfrac{(Z_a+2Z_b)Zc}{Z_a+2Z_b+Z_c} + 2Z_b$$

In order to simplify the calculations, we assumed that Z_1 is a high impedance so that its effect is ignored in the formulations. By combining Eqs. (2) and (3), the relation between the capacitors and inductors at the resonance frequency and the scattering parameters (S_{11} and S_{22}) can be derived (for $Z_o = 50\ \Omega$) as follows.

$$\frac{2L_e\omega L_c}{\frac{(2L_c-2L_eL_c\omega^2)\omega C_c}{2-2\omega^2C_cL_e-\omega^2C_cL_c}+\omega C_c(2L_e+2L_e+L_c)-\frac{4}{\omega}} + j\left\{\frac{L_e\omega}{1-\omega^2\left(\frac{(1-\omega^2L_cC_c)L_c}{2\omega^2L_eC_c+\omega^2L_c-2}+L_e\right)C_c}+\omega L_2-\frac{1}{\omega C_2}-\frac{2}{\omega C_c}\right\}$$

$$= \frac{100}{(1-S_{11})(1-S_{22})-1} \tag{4}$$

The right part of Eq. (4) is a real value. Hence, the imaginary part of the left side should be zero. It is presented by the following equations.

$$\frac{L_e}{-\omega\left(\frac{(1-\omega^2L_cC_c)L_c}{2\omega^2L_eC_c+\omega^2L_c-2}L_e\right)C_c+\frac{1}{\omega}} = \frac{1}{\omega C_2}+\frac{2}{\omega C_c}-\omega L_2 \tag{5}$$

$$0.02L_e\omega L_c[(1-S_{11})(1-S_{22})-1] = \frac{(2L_c-2L_eL_c\omega^2)\omega C_c}{2-2\omega^2C_cL_e-\omega^2C_cL_c}+2\omega C_cL_c-\frac{4}{\omega}+2\omega L_cC_c+\omega L_cC_c \tag{6}$$

Eqs. (5) and (6) describe the values of capacitors and inductors for a minimized insertion loss at a predetermined resonance frequency ($f_r = \omega 2\pi$). Clearly, there is a large degree of freedom to control the insertion loss and control the resonance frequency. Using the proposed resonator, a microstrip triplexer is realized as shown in Figure 2 where its corresponding dimensions are shown in mm. Since we need three transmission paths from port 1 to ports 2, 3, and 4, three resonators are employed. In order to reduce the size, meander lines are used to create the middle channel. Furthermore, optimization experience shows that using the same resonators leads to decrease the isolation between channels. Meanwhile, designing a triplexer with simultaneous close channels, low losses, and high isolation is difficult [22]. Therefore, we decided to make the stubs of the resonator with horizontal coupling different from the others, while the first and last channels created by the same resonator consisting of coupled lines loaded by step impedance cells. Totally, there are five pairs of the coupled lines to create three passbands with improved performance. Similar T-shape structures are employed as feeding lines. This structure is used to optimize the losses and get good impedance matching. The LC equivalent circuit of this type of feeding lines consists of inductors and capacitors that control the ratio of them and can somewhat improve the insertion and return losses. The meander lines with inductive features are loaded inside a resonator to control the second resonance frequency. An increase in the overall lengths of this cell shifts the resonance frequency to the left. The coupled lines at port 3 are placed horizontally to reduce the size. The spiral structures are moved inside the loop to create the middle passband near the first and last channels. The current density distributions of the proposed triplexer at the three resonance frequencies are presented in Figure 3. Since the left loop creates a resonance at 2.66 GHz, the maximum current density is in this loop. In addition, in order to show the effect of high current density parts on the frequency response, three physical dimensions are changed and

the results are shown in Figure 3. One part that has high current density at 2.66 GHz is the microstrip length l_1. Changing this length shifts the first resonance frequency. From Figure 3 it can be seen that by increasing l_1, the first resonance frequency is shifted to the left without changing the other resonance frequencies. The spirals and horizontal coupled lines create the middle channel. As depicted in Figure 3, increasing the physical length l_2 shifts the second resonance frequency to the left. On the other hand, the maximum current density is in the right loop and corresponding coupled lines at 3.43 GHz. Therefore, this loop creates a passband at 3.43 GHz. As shown in Figure 3, increasing the physical length l_3 shifts the third resonance frequency to the left without changing the other resonance frequencies. The isolation between channels as a function of l_1, l_2, and l_3 is also presented in Figure 3. As shown Figure 3, decreasing the lengths l_1, l_2, and l_3 reduces the isolation significantly.

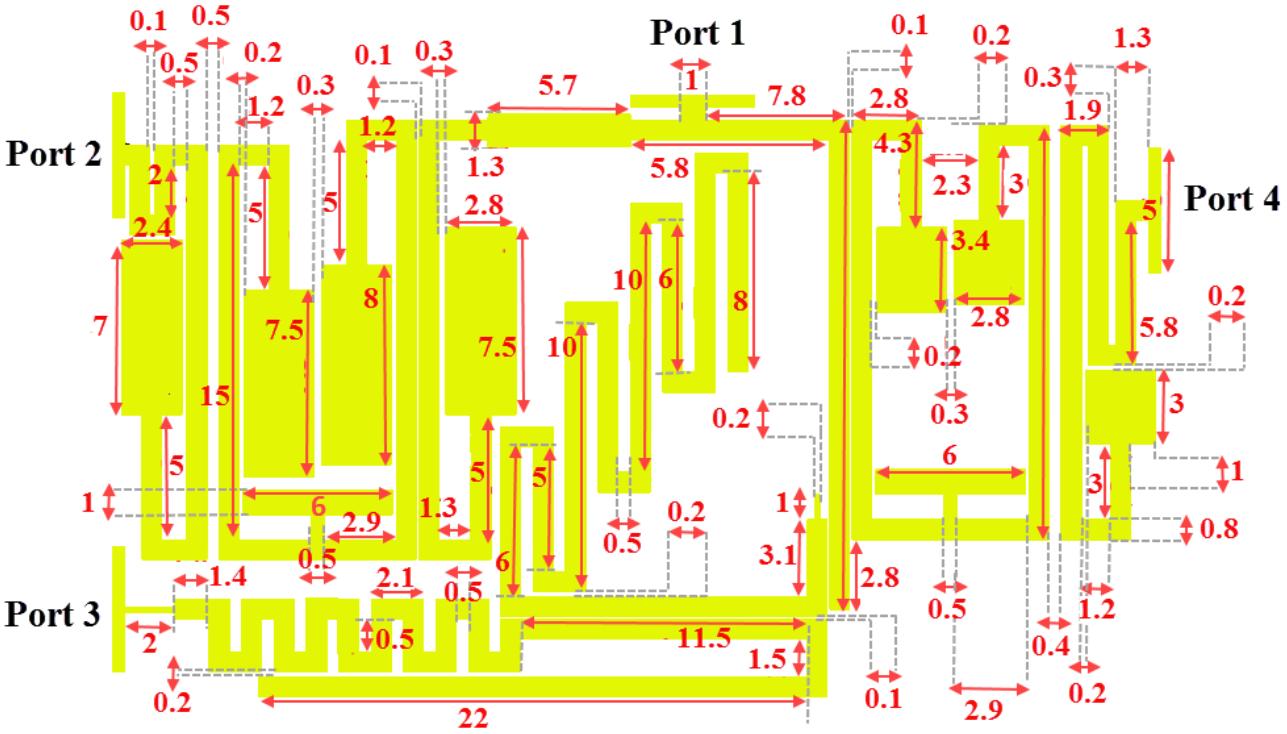

Figure 2. Layout configuration of the proposed triplexer.

As demonstrated in Figure 1b, the proposed resonator consists of a coupled-line loaded by two microstrip step impedance cells of Z_1 and Z_2. On the other hand, the behavior of triplexer stubs (physical lengths l_1 and l_3 and the wider cells connected to them) can be described based on these impedances because the proposed resonator is used in the final triplexer structure. Accordingly, the effects of 1_1 and 1_3 can be explained by the impedance $j\omega L_2$. Hence, we can explain the shifting of resonance frequency using inductor L_2. Inductor L_2 can be extracted from Eq. (5) as follows:

$$L_2 = \frac{L_e}{\omega^2 C_C \left(\frac{(1-\omega^2 L_e C_C) L_c}{2(\omega^2 L_e C_C - 1) + \omega^2 L_c}\right) + \omega^2 L_e C_C - 1} + \frac{1}{\omega^2 C_2} + \frac{2}{\omega^2 C_C} \tag{7}$$

In Eq. (7) C_c is a coupling capacitor such that it is usually a small capacitor in fF. Hence, we can apply some

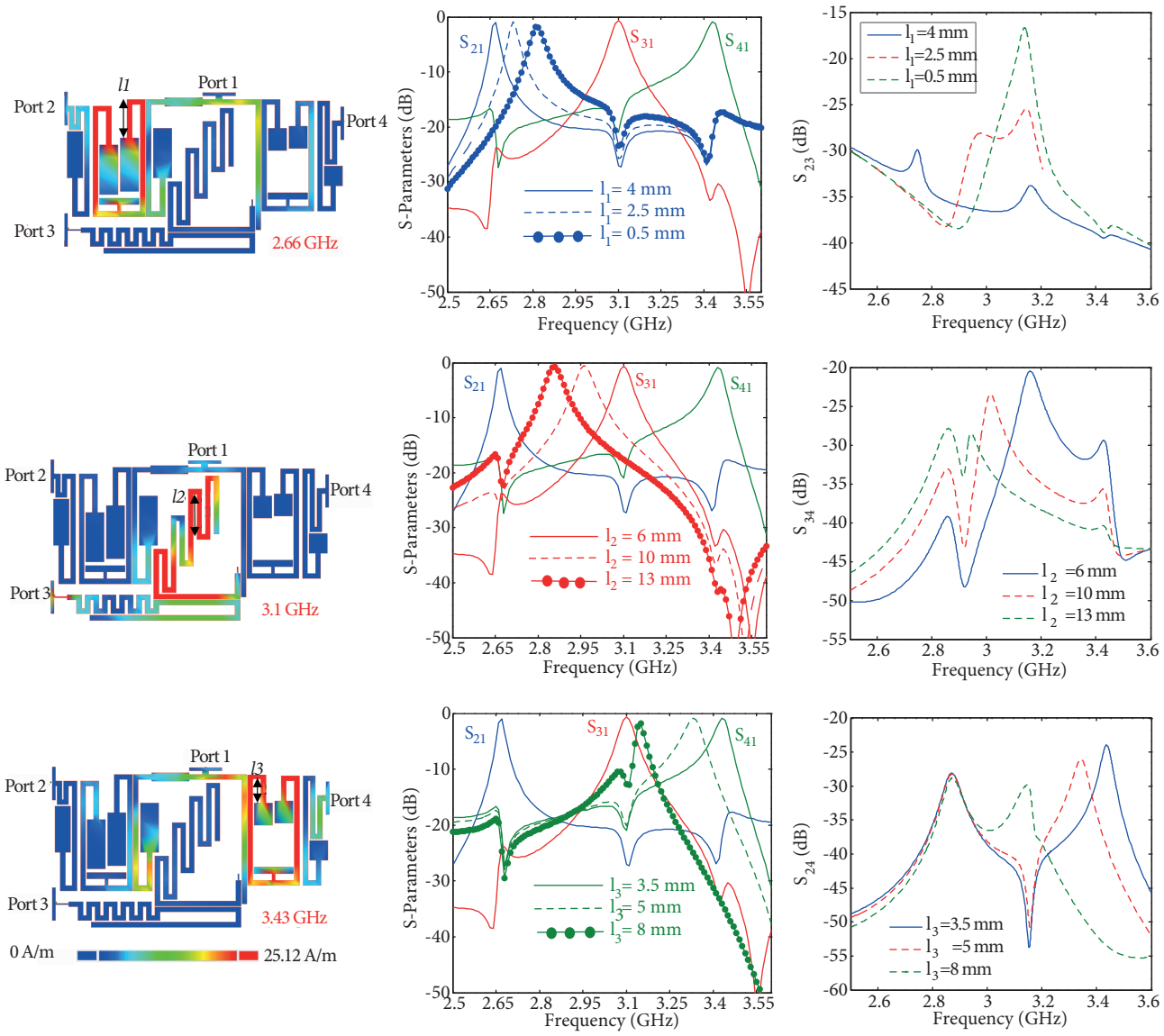

Figure 3. Current density distributions of the proposed triplexer and related curves.

approximations with respect to the ranges of C_c, inductors, and ω. It is clear that the target angular resonance frequency is in GHz. Moreover, based on the resonator structure when L_e and L_c are in nH, we can say that $\omega^2 L_e C_C \langle\langle 1$. Therefore, Eq. (7) can be simplified as follows:

$$L_2 \cong \frac{L_e}{\left(\frac{C_C L_c \omega^2}{-2+\omega^2 L_c}\right) - 1} + \frac{1}{\omega^2 C_2} + \frac{2}{\omega^2 C_C} \Rightarrow L_2 \cong \frac{1}{\omega^2 C_2} + \frac{2}{\omega^2 C_C} - L_e \tag{8}$$

According to Eq. (8), increasing inductor L_2 leads to decrease the resonance frequency. An increase in physical lengths l_1 or l_3 means an increase in L_2, so an increase in physical lengths l_1 or l_3 shifts the resonance frequency to the left. The effect of changing physical length l_2 is similar to that of l_1 and l_3. However, we can replace only an inductor in the equivalent circuit of the meander line. In this case, capacitor C_2 should be removed because this capacitor is an equivalent of the wider cell in the proposed resonator. Removing capacitor

C_2 results in eliminating the term $1/(\omega^2 C_2)$ in Eq. (8). Therefore, $L_2 \cong 2(\omega^2 C_C)^{-1} - L_e$, which shows that increasing physical length l_2 decreases the resonance frequency. According to the above discussion, our mathematical method is in good agreement with the simulation results.

3. Results and discussion

The designed triplexer is simulated by Advanced Design System software using the EM Simulator and fabricated on a substrate of RT_DURROID_5880 with $\varepsilon_r = 2.22$, h = 31 mil, and $\tan(\delta) = 0.0009$. It is measured by Agilent Network Analyzer N5230A. Figure 4a depicts the measured and simulated transmission parameters

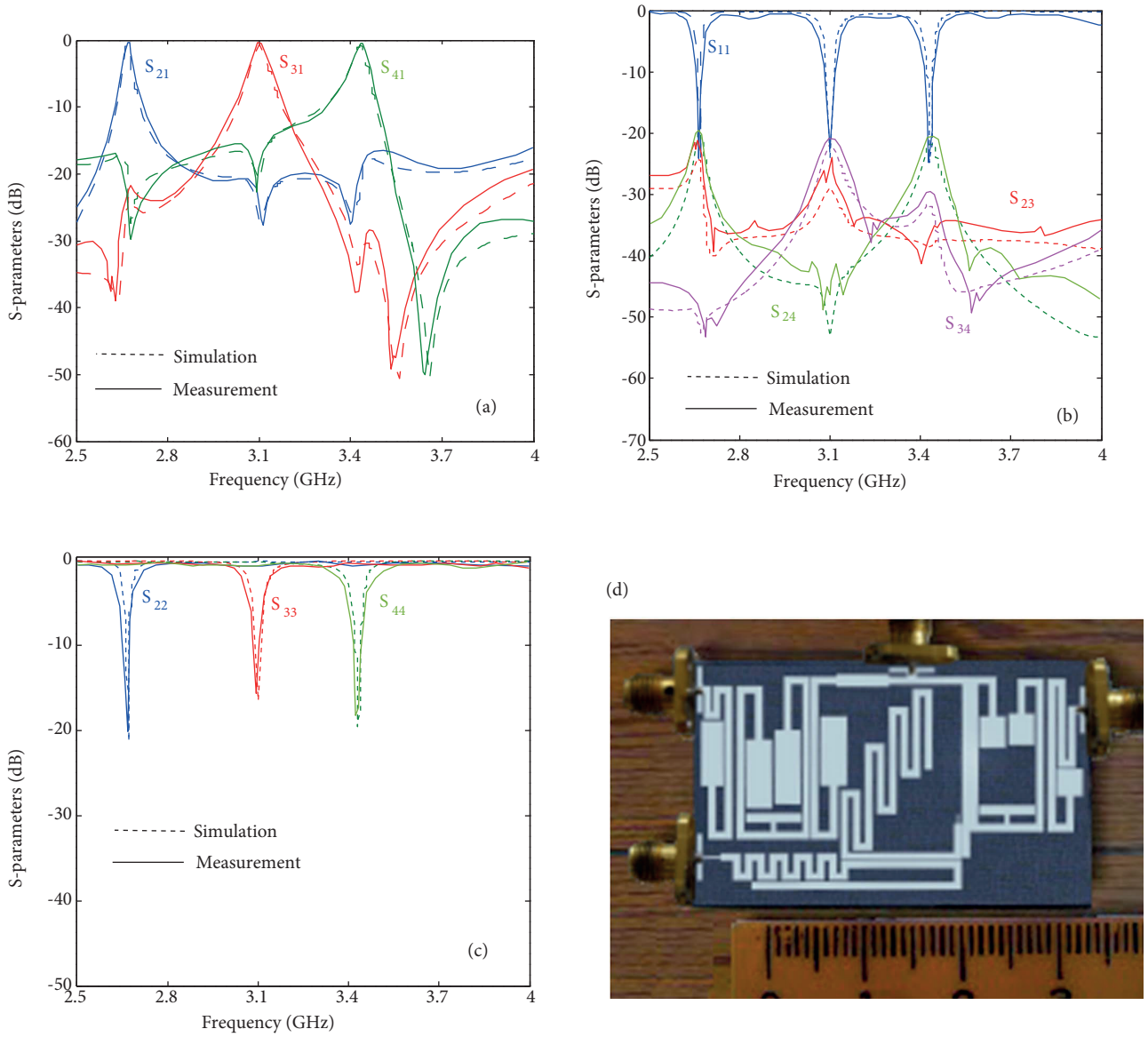

Figure 4. (a) Measured and simulated transmissions; (b) isolation between three ports and input return loss; (c) return losses of ports 2, 3, and 4; (d) a photograph of the fabricated triplexer.

Table. Comparison between the proposed triplexer and previous works.

Ref.	F_{r1}, F_{r2}, F_{r3} (GHz)	IL_1, IL_2, IL_3 (dB)	RL_1, RL_2, RL_3 (dB)	F_{r2}/F_{r1}, F_{r3}/F_{r2}	Size (λg^2)
[3]	0.9, 2.45, 5.35	0.37, 0.68, 0.4	11.8, 21.3, 13.8	2.7, 2.18	0.088
[4]	3.2, 3.7, 4.4	2.7, 2.5, 1.8	16, 16, 16	1.15, 1.19	0.136
[5]	1, 1.25, 1.5	2.7, 1.8, 3.2	15, 15, 15	1.25, 1.2	0.064
[6]	1.4, 1.7,1.9	3.4, 3.5, 3.6	—	1.21, 1.11	0.358
[7]	1.8, 3.1, 4.4	1.97, 1.99, 2.3	24, 22, 25	1.7, 1.42	0.177
[8]	2.05, 2.45, 3.5	1.5, 1.8, 1.5	13, 13, 13	1.19, 1.43	0.346
[9]	3.3, 3.89,4.56	2.2, 2.3, 2.3	14, 14, 14	1.18, 1.17	0.275
[10]	1.21, 1.8, 2.41	1.39, 1.35, 1.27	11.6/14/10	1.48, 1.33	0.055
[11]	1.5, 1.7, 1.9	4.9, 5.8, 5.95	—	1.13, 1.11	0.132
[12]	1, 2.4, 5.8	0.8, 2.1, 2.5	14.5, 12, 12.9	2.4, 2.41	0.067
[13]	1.2, 1.8, 2.4	1.3, 1.3, 1.2	11.6, 14, 10	1.5, 1.33	0.055
[14]	2.4, 3.5, 5.8	0.9, 1.1, 1.3	—	1.46, 1.65	0.119
[15]	0.9, 2.4, 5.5	0.7, 1.7, 1.5	—	2.66, 2.29	—
[16]	3.4, 3.9, 4.4	From 1.6 to 2.2	—	1.14, 1.12	—
This work	2.67, 3.1, 3.43	0.72, 0.63, 0.71	24.5, 24, 24.7	1.16, 1.1	0.137

(S_{21}, S_{31}, and S_{41}). The isolations along with return loss from common input port 1 (S_{11}) are presented in Figure 4b. According to the transmission curves, the proposed triplexer has low insertion losses of 0.72, 0.63, and 0.81 dB at the first, second, and third resonance frequencies, respectively. The isolation levels are better than –20 dB from 2.5 GHz up to 4 GHz. The return losses from ports 2, 3, and 4 (S_{22}, S_{33}, and S_{44}) are presented in Figure 4c. All return losses of the common input port are better than 24 dB. Meanwhile, the return losses from ports 2, 3, and 4 (S_{22}, S_{33}, and S_{44}) are better than 21, 16, and 19 dB, respectively. Figure 4d depicts a photograph of the fabricated triplexer. The overall size of the proposed triplexer is 0.49 λg $\times$ 0.28 λg (42.1 mm $\times$ 23.7 mm), where λ_g is the guided wavelength calculated at 2.67 GHz. The Table illustrates a comparison between this work and the previous reported triplexers. In the Table, the insertion losses and return losses from port 1 are shown with (IL_1, IL_2, IL_3) and (RL_1, RL_2, RL_3), respectively. In addition, the first, second, and third resonance frequencies are shown with F_{r1}, F_{r2}, and F_{r3}, respectively. The Table shows the advantages of our triplexer. Food return losses from all ports are obtained in this work. The best insertion losses were achieved in [3]. Nevertheless, it has low selectivity with undesired common port return losses of 11.8 and 13.8 dB at the first and third passbands, respectively. According to the Table, miniaturization has been carried out in some of the previous works by victimization of the insertion loss [10–13] and return loss [10–14]. References [4,5,10,12–14] have compact sizes but our work has better insertion losses, return losses, and frequency ratios. In comparison with [3], better return losses and frequency ratios are obtained. References [11,16] have good frequency ratios but our design is better in terms of insertion losses and return losses. Meanwhile, with our proposed triplexer, the losses are improved significantly as well as high selectivity being achieved. Another advantage of the proposed triplexer is its low frequency ratios, where designing a triplexer with close resonance frequencies is difficult. The lowest frequency ratio of 1.1 is obtained in this work.

4. Conclusion

In this paper, a novel microstrip triplexer is presented based on a new combination of step impedance cells, spirals, and coupled lines. In addition, a design method is introduced to improve the insertion loss and control

the resonance frequencies so that the insertion losses at all passbands are decreased significantly. Meanwhile, good return losses are obtained at all channels. The design method is based on analyzing the LC equivalent circuit of the proposed resonator. The realized triplexer operates at 2.67 GHz and at 3.1 GHz and 3.43 GHz for GSM (4G) and WiMAX applications, respectively. The passbands are quite close to each other, which makes the proposed triplexer suitable for frequency division duplex applications.

References

[1] Rezaei A, Noori L, Mohamadi H. Design of a novel compact microstrip diplexer with low insertion loss. Microw Opt Techn Let 2017; 59: 1672-1676.

[2] Noori L, Rezaei A. Design of a microstrip diplexer with a novel structure for WiMAX and wireless applications. AEU-Int J Electron C 2017; 77: 18-22.

[3] Zhu C, Zhou J, Wang Y. Design of microstrip planar triplexer for multimode/multi-band wireless systems. Microwave J 2010; 2010: 1-19.

[4] Wu JY, Hsu KW, Tseng YH, Tu WH. High-isolation microstrip triplexer using multiple-mode resonators. IEEE Microw Wirel Co 2012; 22: 173-175.

[5] Chen CF, Shen TM, Huang TY, Wu RB .Design of multimode net-type resonators and their applications to filters and multiplexers. IEEE T Microw Theory 2011; 59: 848-856.

[6] Deng PH, Lai MI, Jeng SK, Chen CH. Design of matching circuits for microstrip triplexers based on stepped-impedance resonators. IEEE T Microw Theory 2006; 54: 4185-4192.

[7] Chinig A, Errkik A, Abdellaoui L, Tajmouati A. Design of a microstrip diplexer and triplexer using open loop resonators. J Microw Optoelectron Electromagn Appl 2016; 16: 65-80.

[8] Sugchai T, Nattapong I, Apirun C. Design of microstrip triplexer using common dual-mode resonator with multi-spurious mode suppression for multiband applications. Appl Mech Mater 2015; 763: 182-188.

[9] Tang CW, Tseng CT. Packaged microstrip triplexer with star-junction topology. Electron Lett 2012; 48: 699-701.

[10] Huang Y, Wen G, Li J. Compact microstrip triplexer based on twist-modified asymmetric split-ring resonators. Electron Lett 2014; 50: 1712-1713.

[11] Lin SC, Yeh CY. Design of microstrip triplexer with high isolation based on parallel coupled-line filters using t-shaped short-circuited resonators. IEEE Microw Wirel Co 2015; 25: 648-650.

[12] Chen FC, Qiu JM, Hu HT, Chu QX ,Lancaster MJ. Design of microstrip lowpass-bandpass triplexer with high isolation. IEEE Microw Wirel Co 2015; 25 :805-807.

[13] Jin X, Yan Z. Microstrip triplexer and switchable triplexer using new impedance matching circuits. Int J Rf Microw C E 2016; 27: 1-9.

[14] Wu HW, Huang SH, Chen YF. Compact microstrip triplexer based on coupled stepped impedance resonators. In: 2013 IEEE MTT-S International Microwave Symposium Digest; 2–7 June 2013; Seattle, WA, USA.

[15] Percaz JM, Chudzik M, Arnedo I, Arregui I, Teberio F, Laso MA, Lopetegi T. Producing and exploiting simultaneously the forward and backward coupling in EBG-assisted microstrip coupled lines. IEEE Antenn Wirel Pr 2015; 15: 873-876.

[16] Karlsson M, Håkansson P, Gong S. A frequency triplexer for ultra-wideband systems utilizing combined broadside- and edge-coupled filters. IEEE T Comp Pack Man 2008; 31: 794-801.

[17] Gorur A, Karpuz C. A novel microstrip triplexer based on meandered loop resonators. In: 2017 IEEE Asia Pacific Microwave Conference; 13–16 November 2017; Kuala Lumpur, Malaysia.

[18] Shairi NA, Sazali MA, Zakaria Z, Ebrahim IM, Zahari MK, Ahmad BH. Hybrid triplexer design using microstrip coupled line resonators for multiband WiMAX front end. In: 2017 7th IEEE International Symposium on Microwave, Antenna, Propagation, and EMC Technologies; 24–27 October 2017; Xi'an, China.

[19] Lo W, Deng PH, Lin CH. Microstrip diplexer and triplexer using mixed directed-feed and coupled-feed line coupled-resonator filters. In: Progress in Electromagnetics Research Symposium - Fall 2017; 19–22 November 2017; Singapore.

[20] Noori L, Rezaei A. Design of a microstrip dual-frequency diplexer using microstrip cells analysis and coupled lines components. Int J Microw Wirel T 2017; 9: 1467-1471.

[21] Hong JS, Lancaster MJ. Microstrip Filters for RF/Microwave Applications. New York, NY, USA: Wiley, 2001.

[22] Noori L, Rezaei A. Design of microstrip wide stopband quad-band bandpass filters for multi-service communication systems. AEU-Int J Electron C 2017; 81: 136-142.